Modeling Spatial Competition and Adaptive Therapy Protocols in Three-Dimensional Vascularized Tumors

by

Sanjana Saurin Shah

A Thesis Presented in Partial Fulfillment
of the Requirements for the Degree
Master of Science

Approved October 2023 by the
Graduate Supervisory Committee:

Joshua J. Daymude, Chair
Stephanie Forrest
Carlo C. Maley

ARIZONA STATE UNIVERSITY

December 2023

ABSTRACT

In contrast to traditional chemotherapy for cancer which fails to address tumor heterogeneity, raises patients' levels of toxicity, and selects for drug-resistant cells, adaptive therapy applies ideas from cancer ecology in employing low-dose drugs to encourage competition between cancerous cells, reducing toxicity and potentially prolonging disease progression. Despite promising results in some clinical trials, optimizing adaptive therapy routines involves navigating a vast space of combinatorial possibilities, including the number of drugs, drug holiday duration, and drug dosages. Computational models can serve as precursors to efficiently explore this space, narrowing the scope of possibilities for in-vivo and in-vitro experiments which are time-consuming, expensive, and specific to tumor types. Among the existing modeling techniques, agent-based models are particularly suited for studying the spatial interactions critical to successful adaptive therapy. In this thesis, I introduce CancerSim, a three-dimensional agent-based model fully implemented in C++ that is designed to simulate tumorigenesis, angiogenesis, drug resistance, and resource competition within a tissue. Additionally, the model is equipped to assess the effectiveness of various adaptive therapy regimens. The thesis provides detailed insights into the biological motivation and calibration of different model parameters. Lastly, I propose a series of research questions and experiments for adaptive therapy that CancerSim can address in the pursuit of advancing cancer treatment strategies.

DEDICATION

I would like to express my gratitude to Garrett, who encouraged me to take a theory class and set off a chain of unexpected events. Your support throughout this thesis means the world to me. This work is dedicated to you.

ACKNOWLEDGMENTS

First and foremost, I want to express my deep gratitude to my advisor, Dr. Joshua Daymude, for entrusting me with the opportunity to contribute to this personally significant project. His guidance not only facilitated the development of my research skills but also provided invaluable support during moments of life-related stress.

I extend my thanks to Dr. Stephanie Forrest and Dr. Carlo Maley for their insights into simulator and experiment design. Dr. Maley's Cancer Evolution and Ecology class created an enriching environment, allowing a computer science major like me to explore the intricacies of cancer treatment.

Special appreciation goes to Walker Mellon, Ariadne Dimarogona, Luis Cisneros, and Kirtus Leyba for their invaluable contributions to designing, calibrating, and visualizing the simulations.

I also want to acknowledge my sister Saniya and my best friends Kalpesh, Stella, Diya, and Parth for being my unwavering support system. Gratitude extends to my family and friends for their consistent encouragement throughout all my endeavors.

Lastly, a heartfelt thank you to everyone, including God, who stood by me during my toughest days and believed in me when self-doubt loomed large. Every achievement I attain is a reflection of your belief in me.

A final note: If you or someone you know is struggling with thoughts of self-harm or suicide, please seek help. Reach out to a mental health professional or a trusted individual in your life. You are not alone, and support is available.

Things get better when you're not looking, but you don't get to see that if you're not here.

TABLE OF CONTENTS

LIST OF TABLES

LIST OF FIGURES

Chapter 1

INTRODUCTION

Traditional chemotherapy aims to eliminate as many cancerous cells as possible by exposing patients to high doses of cytotoxic drugs (Aston et al. 2017). This approach presents several drawbacks, the foremost of which is the heightened cytotoxicity resulting from the administration of chemotherapy drugs at high concentrations, leading to a reduced therapeutic index (Tannock 1998). Additionally, this strategy fails to consider the presence of intratumoral heterogeneity (Marusyk and Polyak 2010), with biopsies detecting only a limited range of heterogeneous populations. Empirical evidence suggests that achieving complete cancer eradication is clinically improbable, frequently culminating in relapse due to the development of drug resistance within the remaining small cluster of cancer cells (Farquhar et al. 2005). This selection for drug-resistant cells leads to the emergence of more aggressive tumors and, tragically, often results in patient fatality attributed to metastatic progression (Marusyk, Janiszewska, and Polyak 2020).

In turn, cancer ecology and evolution present a new way to look at cancer development and treatment (Adler and Gordon 2019). Each distinct clonal cell group within the tumor micro-environment can be likened to a unique species within an ecosystem (Aktipis and Nesse 2013). The interactions, both within and among these "species," shed light on the mechanisms underlying tumorigenesis and offer valuable insights into therapeutic strategies that leverage these interactions to combat cancerous cells (Korolev, Xavier, and Gore 2014). This approach implements a *treatment for stability*

strategy, where the objective is to enable patients to coexist with cancer rather than seeking complete eradication (F. Thomas et al. 2018).

One innovative treatment strategy, informed by cancer ecology, is *adaptive therapy*, which aims to curtail the proliferation of drug-resistant cells by employing low-dose drugs to facilitate competition between *resistant* and *sensitive* cells for vital resources, thereby maintaining a manageable tumor size (Gatenby et al. 2009). This approach operates under the assumption that developing drug resistance comes at a cost to the cell's other functions, reducing their overall fitness (Gatenby 2009). While the resistant cells may gain a selective advantage during drug administration, this advantage is offset in the absence of drugs, where sensitive cells exhibit greater efficiency in reproduction (Enriquez-Navas et al. 2016). Furthermore, adaptive therapy advocates for the use of significantly lower drug doses than the Maximum Tolerated Dose (MTD), reducing the cytotoxicity experienced by the patient (Zhang et al. 2017).

Currently, ongoing human trials and mouse models are exploring the efficiency of adaptive therapy in controlling cancer progression. One of the early human trials focused on Abiraterone treatment for metastatic castrate-resistant cells (Zhang et al. 2017). This trial reported a significantly longer Time to Progression (TTP) for adaptive therapy protocols (at least 27 months) compared to standard dosing (median TTP of 16.5 months) while also reducing drug use by 46% (Enriquez-Navas et al. 2016). Additionally, several mouse models also seem to suggest this trend (Gatenby et al. 2009; Kam et al. 2014; Enriquez-Navas et al. 2016).

These trials highlight the advantages of adaptive therapy over traditional chemotherapy, however, several factors need to be considered before suggesting treatment decisions (West et al. 2023). Identifying adaptive therapy routines that effectively exploit cancer ecology involves navigating a vast space of combinatorial possibilities,

including the number of drugs, drug holiday duration, and drug dosages (Metzcar et al. 2019). Ultimately, conducting in-vivo and in-vitro experiments would provide the most accurate results when exploring this extensive array of potential regimens. However, they are time-consuming, costly, and often specific to tumor types and sub-types (Trisilowati and Mallet 2012). In this context, computational models can serve as valuable tools to narrow the scope of laboratory experiments (McDonald et al. 2023).

In this thesis, we present CancerSim, a three-dimensional agent-based model designed to simulate angiogenesis and neoplastic progression along with spatial competition for resources between different cell populations in the presence and absence of drugs. This model can be used to examine ecological hypotheses about the dynamics of cooperation and competition among diverse cell populations within a tumor, particularly under the influence of distinct drug treatment protocols.

In Chapter 2, we survey existing computational models for cancer treatment. In Chapter 3, we define our model and biologically align/calibrate its parameters in Chapter 4. In Chapter 5, we present some research questions that CancerSim is well-suited to answer. Lastly, we conclude this study with directions for future work in Chapter 6.

Chapter 2

RELATED WORK

Computational models assist in reducing the scope of in-vivo and in-vitro experiments, allowing observation at different levels of abstraction and flexible parameter changes (Trisilowati and Mallet 2012; Metzcar et al. 2019). In cancer research, they address different aspects of tumorigenesis like interactions between pre-cancerous cells and host immune cells, hypoxia in breast cancer, and the turnover rate's impact on treatment outcomes (Mallet and De Pillis 2006; Norton et al. 2017; Strobl et al. 2021). These models can efficiently explore parameter landscapes, particularly for challenging biological characteristics (Yu and Bagheri 2020).

The sheer number of possibilities for an adaptive therapy protocol makes it a good candidate for pre-clinical trials on computational models. The model by Gatenby et al. 2009 highlighted the effectiveness of a treatment-for-stability approach and was validated through subsequent in-vivo experiments (Gatenby et al. 2009). Various other adaptive therapy models, like those using Ordinary Differential Equations (ODE), explore growth and resistance development in different tumor microenvironments (Bacevic et al. 2017; Strobl et al. 2021; Angelini et al. 2022). However, ODEs, assume well-mixed cell populations (Beerenwinkel et al. 2015), which may not accurately represent solid tumors (Swanton 2012). In fact, spatial diversification of resistant cells has a significant impact on treatment outcomes and thus is an important modeling attribute (Wu et al. 2022).

Agent-based models (ABMs) are ideal for capturing spatial distributions in computational modeling (McDonald et al. 2023). These models center on individual

agents (cells) in a simulated space and govern their interactions based on specific rules, unveiling complex system behaviors and emergent effects (Bonabeau 2002). ABMs have been used to explore various factors influencing adaptive therapy outcomes, such as spatial distribution of resistant cells (Strobl et al. 2022), multi-drug adaptive therapy (D. S. Thomas et al. 2022), and dose modulation efficiency (Gallaher et al. 2018). While ABMs provide real-time insights into tumor dynamics, they come with application-specific strengths and limitations, from tumor type restrictions (Norton et al. 2017) to the focus on two-dimensional models overlooking distinctions from three-dimensional counterparts (Baker and Chen 2012).

CancerSim1.0 was originally introduced to study the acquisition of hallmarks of cancer (Hanahan and Weinberg 2011) by cells in a tissue and their progression to metastatic tumors (Abbott, Forrest, and Pienta 2006). It was a three-dimensional ABM that handled angiogenesis and spatial heterogeneity in the distribution of resources. However, it had some limitations, including biological inconsistencies, and a lack of resource conservation from the vasculature. Additionally, it did not model drug resistance or drug delivery, making it inadequate for effective adaptive therapy modeling. CancerSim2.0 (referred to as CancerSim in this thesis), builds off CancerSim1.0 and addresses these issues, as we will discuss in the following sections.

Chapter 3

MODEL DESIGN

In this chapter, we present the model design for CancerSim, a three-dimensional ABM, designed to simulate interactions between vasculature and cells in a tissue in the presence of different drug combinations and dosage regimens, encompassing tumorigenesis and drug distribution dynamics.

3.1 Modeling Space

In CancerSim, the simulated space takes on a spherical shape whose volume is determined by the desired number of cell locations (N). Cell and capillary locations within this sphere are represented as spheres in a *face-centered cubic lattice* (FCC), where each lattice location, excluding boundary spaces, has 12 equidistant neighbors. Within this environment, each lattice location can contain a single cell or remain unoccupied, while capillaries can co-locate with cells. Figure 1 illustrates a sample tissue in CancerSim where the blue cells are the sensitive cells, and the green cells are the resistant cells. The vasculature is represented by the tree in the center with black edges, and the nodes representing the capillary locations. Also, for a sense of scale, the distance between adjacent cells corresponds to 15 μm in real-world terms. This three-dimensional spatial framework is essential for understanding spatial heterogeneity, resource distribution, and the organization of sensitive and resistant cells, which play important roles in the success of adaptive therapies (Strobl et al. 2022).

Because of the shape of the face-centered cubic lattice, the radius R of the tissue

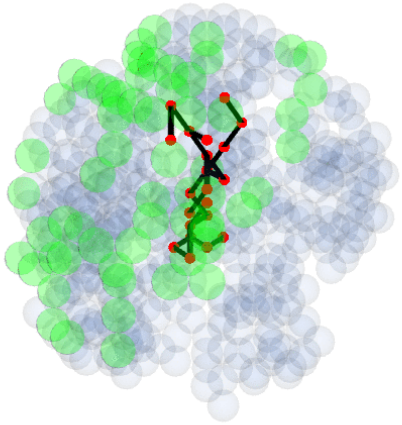

Figure 1. CancerSim Tissue

is given by:

$$R = \text{ceil}\left(\frac{\sqrt[3]{3 \cdot N \cdot \frac{\sqrt{2}}{\pi}}}{2}\right) \tag{3.1}$$

3.2 Modeling Time

CancerSim employs a discrete event model combined with discrete time steps to systematically schedule events at predefined future time intervals. This modeling approach treats the system's operation as a sequence of distinct events occurring at specific points in time, marking changes in the system's state (Robinson 2004). Additionally, the system state between two time steps remains fixed and each time step corresponds to 1 hour of real time.

This discrete event model handles three types of events: drug events (3.4), capillary events (3.5), and cell events (3.6).

3.3 Resource Dynamics

3.3.1 Diffusion and Resource Flow

CancerSim models resources (i.e., nutrients, drugs, and angiogenesis factor) being released by *point sources* and being absorbed by *point sinks* according to the *diffusion equation*, or Fick's second law:

$$\frac{\partial C(\vec{x},t)}{\partial t} = D \cdot \nabla^2 C(\vec{x},t), \tag{3.2}$$

where $C(\vec{x},t)$ is the concentration of a given resource at location $\vec{x}$ at time t, $D > 0$ is the resource's diffusion constant, and ∇^2 is the Laplacian generalizing the one-dimensional second derivative for our three-dimensional setting. The time scale of diffusion is much faster than our hour-long time steps, so we analyze diffusion at steady-state in the inhomogeneous case when $S(\vec{x})$ are the fixed rates of concentration production at locations $\vec{x}$. This is written as a Poisson equation:

$$\nabla^2 C(\vec{x},t) = -\frac{S(\vec{x})}{D}. \tag{3.3}$$

We are particularly interested in $S(\vec{x})$ as a collection of point sources and sinks at locations $(\vec{s}_1,\ldots,\vec{s}_m)$ that release or absorb resources at fixed rates $(C_1,\ldots,C_m)$, respectively. These sources and sinks can be represented as Dirac delta functions δ:

$$\nabla^2 C(\vec{x},t) = -\frac{1}{D} \cdot \sum_{i=1}^{m} C_i \cdot \delta(\vec{s}_i). \tag{3.4}$$

Resource	**Source**	**Sink**
Nutrients	Capillaries	Cells
Drugs (when active)	Capillaries	Cells
Angiogenesis Factor	Cells (when starving)	None

Table 1. Resource Interactions in CancerSim

The solution to this equation is given by a superposition of Green's functions:

$$C(\vec{x}, t) = \frac{1}{D} \cdot \sum_{i=1}^{m} \frac{C_i}{4\pi \cdot ||\vec{x} - \vec{s}_i||_2}. \tag{3.5}$$

implying that resource concentration at a given location is determined by its proximity to point sources and sinks, leading to spatial heterogeneity in resource distribution. This solution is analogous to the "steady-source" version of the heat equation with multiple sources or sinks; see Chapter XV of (Carslaw and Jaeger 1959). A summary of sources and sinks for different resources in CancerSim is provided in Table 1.

3.3.2 Stochastic Thresholds

Various capillary and cellular processes like mitosis, angiogenesis, and drug-induced death depend on the concentration of resources at the cell/capillary's location. These processes are triggered based on stochastic thresholds using the sigmoidal function:

$$f(x; m, k) = \frac{1}{1 + e^{-k(x-m)}} \tag{3.6}$$

where $f(x; m, k) \in (0, 1)$ is the probability of a process being triggered at the concentration x, k is the steepness of the function and m is the concentration value at which the probability of having a process triggering is exactly $1/2$. While the likelihood of

an event occurring increases with rising resource concentrations, the introduction of stochastic thresholds mirrors the inherent noise in biological systems.

CancerSim models three processes using stochastic thresholds. The likelihood of a cell mitosis is determined with a stochastic threshold function $f_n(x_n; m_n, k_n)$, where x_n is the concentration of nutrients at the cell's location. Similarly, the likelihood of drug death in a cell is decided by the stochastic threshold $f_d(x_d; m_d, k_d)$, where x_d is the drug concentration at the cell's location. Lastly, a capillary performs angiogenesis when $f_a(x_a; m_a, k_a)$ function returns true, where x_a is the concentration of angiogenesis factor (AF) at the capillary's location. The calibration for the mean and steepness constants for these functions is addressed in Chapter 4.

3.4 Drugs

Drug events in CancerSim update a specific drug at a specific dosage at a specific time step. A drug routine in turn maintains a list of such events and is provided as an input to the simulation. CancerSim supports the inclusion of multiple drugs, which can be administered together or separately with their respective doses. These features enable diverse adaptive therapy strategies, including drug modulation (changing the concentration of the drug over time), holidays (discontinuing drug administration for a given period), cycling (switching between multiple drugs), drug cocktails (administering multiple drugs at the same time), and any combination thereof.

Active drugs can eliminate sensitive cells before they can perform mitosis, with cell death likelihood determined by a stochastic threshold function $f_d(x_d; x_d, k_d) \in (0, 1)$ on drug concentration (Eq. 3.6). Drug resistance in cells is explained further in Section 3.6.

3.5 Vasculature

In CancerSim, the vasculature supplies all nutrients and drugs to the rest of the tissue. It is composed of capillaries organized as a branching tree rooted at a source capillary located at the center of the tissue. During a vasculature event, a leaf capillary in this tree attempts angiogenesis which, if successful, will cause the capillary to *elongate* into an adjacent position or *branch* into two adjacent positions.

A vasculature event is thus an opportunity for the given capillary to perform angiogenesis, and improve the distribution of resources in the simulation space.

A capillary executing a vasculature event needs to determine whether it should perform angiogenesis based on the outcome of the stochastic threshold $f_a(x_a; m_a, k_a) \in (0, 1)$ where the likelihood of performing angiogenesis increases with the AF concentration (x_a) at that capillary location. At this point, if the capillary does not perform angiogenesis, it schedules another event t_{cap} time steps in the future.

If it passes the stochastic AF threshold for angiogenesis, the capillary faces the second decision: whether to branch or elongate. This choice depends on a probability $p_b \in (0, 1)$, where p_b represents the probability of branching, and $1 - p_b$ represents the probability of elongation.

After this choice, the capillary determines the direction for new capillary growth based on the surrounding AF concentration. Since AF is produced by starving cells, it forms a concentration gradient that points toward the direction of maximum nutrient demand. Thus, the direction of angiogenesis is determined through a weighted probability based on the AF concentration at each neighboring location i.

$$\Pr(direction = i) \propto \frac{x_{ai}}{\sum_{i=1}^{12} x_{ai}} \tag{3.7}$$

where x_{ai} is the AF concentration at the location of neighbor i. For branching, this decision process is performed twice (for two branches).

After branching or elongation, each newly formed capillary schedules a future capillary event t_{cap} time steps in the future. However, each capillary is limited to branching or elongating only once, preventing the parent capillary from undergoing angiogenesis again.

When a capillary with a point source concentration of C_0 divides, it remains a point source for $C_0 \cdot \varepsilon$ concentration, with the remaining $1 - \varepsilon$ fraction distributed among its descendants. In elongation, the new capillary has a point source concentration of $C_0 \cdot (1 - \varepsilon)$, while in branching, each branch has a concentration of $C_0 \cdot \frac{(1-\varepsilon)}{2}$. This ensures that the sum of the relative concentration of all capillaries consistently equals 1. This branching and elongation model conserves the total concentration of nutrients and drugs entering the system, regardless of the number of capillaries.

3.6 Cells

In CancerSim, cells possess a phenotype defined by a set of cancer hallmarks (Hanahan and Weinberg 2011) and drug resistances that determine their fitness and drive competition. It is important to note that drug resistances are specific to individual drugs, meaning a cell may be resistant to one drug but sensitive to another.

Every time a scheduled cell event is executed in CancerSim, the cell undergoes a cycle. First, the cell checks if it is actually alive. It could have been exposed to non-specific causes of death or exhausted its telomeres. Additionally, it could have reached a (stochastic) threshold concentration of drugs it is sensitive to. Drug resistance is then modeled by increasing the m_d parameter for $f_d(x_n; m_d, k_n)$, which

increases the amount of concentration required to trigger drug death, serving as a fitness advantage. Following these checks, if the cell is not dead, then it proceeds with the rest of the cell cycle.

The cell exits its G_0 resting phase and enters the G_1 phase where it checks if it has sufficient nutrients for mitosis. Different types of cells have different nutrient requirements based on the number of drug resistances they have because gaining drug resistance comes at the cost of higher nutrient requirements. If a cell has $r \geq 0$ drug resistances, then its nutrient requirement increases by r units. In case it does not have sufficient nutrients, it becomes an AF source, reenters the G_0 phase, and schedules a later event t_{cell} time steps in the future. If the cell has the Sustained Angiogenesis hallmark, then it always produces AF, which is modeled in CancerSim by making them constant sources of AF regardless of whether they have sufficient nutrients.

On passing the G_1 phase, it reaches the G_1 Checkpoint. Biologically, at this point, the cell requires sufficient nutrients and the presence of self-growth factors to continue with mitosis. CancerSim represents self-growth signals inside a central spherical region, and cells with Sustained Proliferative Signaling (SPS) hallmark can expand beyond this region, unlike normal cells. Thus, if a cell has sufficient nutrients and is in the self-growth signal region (or has the SPS hallmark), it enters the S phase.

During the S Phase, the cell's DNA is replicated, and at this point each hallmark or resistance that the cell does not already have is obtained with probability p_m. If a cell has the Genetic Instability hallmark, then it mutates with the probability $p_m = min(p_m * g, 1)$, for some $g > 1$. Note that in CancerSim, cells accumulate hallmarks and resistances, but do not lose them, and these phenotypes are always inherited by their descendants.

After the S phase, the cell must pass the first part of the G_2 checkpoint that checks

for DNA damage that might have occurred during the S Phase. The probability of a hallmark or drug resistance being detected is controlled by the parameter p_d. If a hallmark or drug resistance is detected, the cell undergoes apoptosis. If the cell has the Evading Apoptosis hallmark, then it always passes this check and all hallmarks or drug resistances go undetected.

On passing the first part of the G_2 checkpoint, the cell reaches the second part of the G_2 checkpoint where it looks for sufficient space to divide. For a cell to divide, it needs at least one empty neighboring location in the lattice for one of the daughter cells, while the other takes the position of the parent. If the cell has an empty neighboring location, it proceeds to the M phase. On the other hand, if the cell does not have an empty neighboring location but has the Evading Contact Inhibition hallmark, it can kill a neighboring cell with probability p_r to make space for the new daughter cell and clear the G_2 checkpoint.

During the M Phase, the cell divides into two cells, and schedules later cell events for both the daughter cells. At this point, if the cells have the Replicative Immortality hallmark, they do not exhaust their telomeres and can keep dividing indefinitely, while, if they do not have the Replicative Immortality hallmark, then their telomeres decrease in length.

Chapter 4

CALIBRATION

CancerSim must be calibrated to ensure a reasonable level of biological accuracy and relevance of its predictions. This chapter details the reasoning behind all calibration decisions and parameter values. A summary of all the parameters and their calibrations is given in Table 2.

4.1 Event and Simulation Intervals

Recall from Section 3.2 that our fundamental unit of time is a *time step* representing one hour of real-time. In these units, we have the following durations:

- At the end of a cell cycle, the cell schedules its next event for $t_{cell} \sim \mathcal{N}(\mu = 48, \sigma = 8)$ steps in the future, a normally distributed random value with a 48-hour mean and 8-hour standard deviation. This is calibrated based on an average cell cycle length of 1–3 days.
- When a new capillary is formed or an existing one has insufficient AF to initiate angiogenesis, it schedules its next vasculature event for $t_{cap} \sim \mathcal{N}(\mu = 96, \sigma = 8)$ steps in the future, a normally distributed random value that is twice the duration of the average cell cycle.
- The total simulation time is $T = 43{,}830$ steps, which is approximately equal to five years, the duration of some longer-running clinical trials for adaptive therapy (Zhang et al. 2017).

Parameter	Description	Value / Computation
R	Radius of the simulated tissue	Calculated during runtime using Eq. 3.1
t_{cell}	Duration of a cell life cycle	$\mathcal{N}(\mu = 48, \sigma = 8)$ timesteps
t_{cap}	Duration of a capillary life cycle	$\mathcal{N}(\mu = 96, \sigma = 8)$ timesteps
m_n	Midpoint for cell mitosis stochastic threshold function	-0.1
k_n	Steepness constant for cell mitosis stochastic threshold function	45.95
ε	Retention Factor; the fraction of point source concentration retained by a parent capillary after angiogenesis	Computed during runtime based on Eq. 4.7
C_n	Nutrient concentration that is sufficient to provide nutrients to all the cells in the simulation	Computed during runtime based on Eq. 4.1
D_n	Nutrient Diffusion Constant	1
m_d^s	Midpoint for the stochastic threshold function for drug death in sensitive cells	-0.459
m_d^r	Midpoint for the stochastic threshold function for drug death in resistant cells	4.82
k_d	Steepness constant for the stochastic threshold function for drug death	14.33
D_d	Drug Diffusion Constant	1
m_a	Midpoint for AF stochastic threshold function	11.425
k_a	Steepness constant for AF stochastic threshold function	0.40
D_a	AF Diffusion Constant	0.12

Table 2. Parameters in CancerSim

4.2 Nutrient Diffusion

In this section, we calibrate parameters controlling the diffusion of nutrients released by the vasculature and absorbed by the cells. Specifically, we must calibrate the midpoint m_n and steepness k_n of cells' stochastic threshold for mitosis, the fraction of resources ε retained by capillaries during angiogenesis, the diffusion constant D_n of nutrients, and the total concentration of nutrients provided by the vasculature C_n.

We parameterize the sigmoid function $f_n(x; m_n, k_n) \in (0, 1)$ defining the stochastic threshold for mitosis such that a sensitive cell has a 99% chance of mitosis when the concentration of nutrients at its position is zero (i.e., the cell has exactly the nutrients it requires) and a 50% chance of mitosis when the concentration is -0.1 (i.e., 90% of sufficient nutrients). This yields midpoint $m_n = -0.1$ and steepness $k_n \approx 45.95$.

Next, we calibrate the capillary retention factor ε. Precisely adjusting ε is essential for achieving a resource distribution in the system that facilitates competition among cells, avoiding both resource scarcity and excessive nutrient availability. Typically, capillaries can effectively support cells within 50–100 μm depending on tissue density and vasculature structure. We calibrate ε such that, even if the entire tissue is filled with cells acting as nutrient sinks, (1) the source capillary at the tissue's center provides sufficient nutrients for mitosis to any cell within a 100 μm radius and (2) a capillary at the tissue's boundary provides sufficient nutrients for mitosis to any cell within a 50 μm radius. Following the steady-state concentrations given by Eq. 3.5 and letting $\vec{x}_{100}$ be the position of any cell exactly 100 μm from the center, the first condition can be formulated as:

$$\frac{1}{D_n}\left(\frac{\varepsilon \cdot C_n}{4\pi \cdot ||\vec{x}_{100}||_2} - \sum_{\vec{x}\neq\vec{x}_{100}} \frac{1}{4\pi \cdot ||\vec{x}_{100} - \vec{x}||_2}\right) = 0. \tag{4.1}$$

Analogously, letting $\vec{x}_{bnd}$ be the position of any capillary at the tissue's boundary and

$\vec{x}_{50}$ be the position of any cell exactly 50 μm from this capillary, the second condition can be formulated as:

$$\frac{1}{D_n}\left(\frac{(1-\varepsilon)^R \cdot C_n}{G_n(R,p_b)\cdot 4\pi\cdot||\vec{x}_{50}-\vec{x}_{bnd}||_2} - \sum_{\vec{x}\neq\vec{x}_{50}} \frac{1}{4\pi\cdot||\vec{x}_{50}-\vec{x}||_2}\right) = 0, \tag{4.2}$$

where R is the radius of the tissue, $(1-\varepsilon)^R \cdot C_n$ is the total point source concentration of nutrients summed over all capillaries at depth R in the vasculature, and $G_n(R,p_b)$ is the expected number of capillaries at depth R in the vasculature given a branching probability p_b. Throughout, we set $p_b = 0.25$ (i.e., the vasculature branches every four capillaries, on average) since this does not overcrowd the system with branches but also ensures branching does occur reasonably often, even within smaller system sizes.

With our fundamental unit of space (one cell location) equaling 15 μm, we have $||\vec{x}_{100}||_2 = (100/15)$ and $||\vec{x}_{50}-\vec{x}_{bnd}||_2 = (50/15)$. Dividing Eq. 4.1 by Eq. 4.2 after rearranging terms, we obtain

$$\frac{\varepsilon}{(1-\varepsilon)^R} = \alpha := \frac{2\cdot\sum_{\vec{x}\neq\vec{x}_{100}} \frac{1}{||\vec{x}_{100}-\vec{x}||_2}}{G_n(R,p_b)\cdot\sum_{\vec{x}\neq\vec{x}_{50}} \frac{1}{||\vec{x}_{50}-\vec{x}||_2}}. \tag{4.3}$$

The right-hand side α of Eq. 4.3, although cumbersome, can be computed given the number of cell locations N and the branching probability p_b. The left side, however, cannot be solved algebraically. We instead apply a second-order approximation:

$$\frac{\varepsilon}{(1-\varepsilon)^R} \approx \varepsilon\cdot e^{R(\varepsilon+\varepsilon^2/2)} = \varepsilon\cdot e^{\varepsilon(R+R\varepsilon/2)}. \tag{4.4}$$

Our goal is to fit this approximation to a form $xe^x = y$ so that we can use the principal branch of a Lambert W function to obtain a value $x \approx W_0(y)$. Applying Eq. 4.4 to Eq. 4.3 and multiplying both sides,

$$\alpha\cdot\left(R+\frac{R\cdot\varepsilon}{2}\right) \approx \varepsilon\cdot\left(R+\frac{R\cdot\varepsilon}{2}\right)\cdot e^{\varepsilon(R+R\varepsilon/2)}. \tag{4.5}$$

Setting $x = \varepsilon \cdot (R + R\varepsilon/2)$ and observing that $x \to 1$ as $\varepsilon \to 0$ implies

$$\varepsilon \cdot \left(R + \frac{R \cdot \varepsilon}{2} \right) \approx W_0(\alpha \cdot R), \tag{4.6}$$

and rearranging terms, we finally obtain:

$$\varepsilon \approx \frac{\sqrt{R^2 + 2 \cdot R \cdot W_0(\alpha \cdot R)}}{R} - 1 \tag{4.7}$$

Total Nutrient Requirement (C_n) represents the total nutrient concentration needed to support all cells in the system, assuming they are all sensitive and occupy the entire tissue. This is calculated by solving Eq. 4.1, which takes the form:

$$C_n = \left(\sum_{\vec{x} \neq \vec{x}_{100}} \frac{1}{||\vec{x}_{100} - \vec{x}||_2} \right) \cdot \frac{||\vec{x}_{100}||_2}{\varepsilon} \tag{4.8}$$

Nutrient Diffusion Constant (D_n) is a measure of how quickly nutrients spread or diffuse through a medium in unit time. From Eq. 4.1 and Eq. 4.2, we can conclude that D_n can have any positive value to match our constraints, and for the sake of simplicity, we set $D_n = 1$.

4.3 Diffusion of Drugs

In this section, we calibrate parameters controlling the diffusion of drugs released by the vasculature and absorbed by the cells. Specifically, we must calibrate the midpoint m_n and steepness k_n of cells' stochastic threshold for drug death, the diffusion constant D_d of drugs, and the maximum total dose of drugs provided by the vasculature C_{MTD}.

We parameterize the sigmoid function $f_d(x_d; m_d, k_d) \in (0, 1)$ defining the stochastic threshold for cell drug death, utilizing Table 2 of Nowacka et al. 2021 to derive midpoints m_d depending on whether a cell is resistant. In that study, the IC_{50} values

for Paclitaxel are reported as $\mu_s \pm \sigma_s = 3{,}737 \pm 1{,}055$ $(\text{ng/ml})^2$ for sensitive cells and $\mu_r \pm \sigma_r = 40{,}382 \pm 4{,}110$ $(\text{ng/ml})^2$ for resistant cells.

We normalize the sensitive cells' normal distribution into our range of $[-1, 0]$ (i.e., the range of a cell absorbing no nutrients to absorbing a lethal dose) by mapping $0 \to -1$ and $\mu_s + 3\sigma_s \to 0$, yielding the sigmoid midpoint $\mu_s \to m_d^s \approx -0.459$ and steepness $k_d \approx 14.33$ for sensitive cells. For resistant cells, we keep the same steepness but shift the midpoint $m_d^r = (\mu_r/\mu_s) \cdot (m_d^s + 1) - 1 \approx 4.82$.

We know from Eq. 4.1 and Eq. 4.2 that the value of the diffusion constant can be any arbitrary positive value, and thus we set $D_d = D_n = 1$. While drug concentration can vary depending on the dosage, we estimate the maximum tolerated dose (MTD) of drugs as whatever concentration could effectively kill 10% of all cells since 10% weight loss is a standard approximation of MTD (van Berlo et al. 2022). Since all cells have unit sink concentration, we set $C_{MTD} = (0.1) \cdot C_n$.

4.4 Diffusion of Angiogenesis Factor

In this section, we calibrate parameters controlling the diffusion of AF released by the cells and sensed (but not absorbed) by the capillaries. Specifically, we must calibrate the midpoint m_a and steepness k_a of capillaries' stochastic threshold for angiogenesis, and the diffusion constant D_a of AF.

We parameterize the sigmoid $f_a(x_a; m_a, k_a) \in (0, 1)$ defining the stochastic threshold for angiogenesis. The literature is not conclusive on angiogenesis thresholds, so we instead implement a heuristic based on the number of cells within one unit distance outside the 100 μm support range of a capillary; in CancerSim's FCC lattice, this count is $N_{>100} = 914$. We choose the sigmoid's parameters such that when 25% (resp.,

12.5%) of the $N_{>100}$ cells are secreting AF, the capillary has a 99% chance (resp., 50%) of angiogenesis. This yields $m_a = N_{>100} \cdot 12.5\% \cdot 0.1 = 11.425$ and $k_a \approx 0.40$.

Each cell source of AF secretes a unit amount of concentration, $c_{AF} = 1$. We calibrate the AF diffusion constant D_a such that a cell secreting AF from just beyond a capillary's 100 μm support range contributes 0.1 concentration to that capillary's gradient value. Note that any concentration contribution $\ll 1$ would suffice here, as it just updates the D_a required, as shown in the below calculations.

$$\frac{c_{AF}}{D_a \cdot 4\pi \cdot (100/15)} = 0.1 \quad \Rightarrow \quad D_a = \frac{1}{0.1 \cdot 4\pi \cdot (100/15)} \quad \Rightarrow \quad D_a \approx 0.12 \tag{4.9}$$

Chapter 5

EXPERIMENTS

In this chapter, we present different experiments and related research questions regarding adaptive therapy that CancerSim is well-suited to answer with its three-dimensional modeling of resource competition, angiogenesis, and neoplastic progression.

5.1 Experiments

5.1.1 Optimal Drug Duration - Drug Holiday Periods in an Adaptive Therapy Protocol

Drug holidays help mitigate the cytotoxic effects of treatment and allow the sensitive cells to recover and compete with drug-resistant counterparts for vital resources (Garattini et al. 2021). However, it is important to find the right balance for the duration of these drug holidays. An excessively long drug holiday is akin to discontinuing therapy, while a too-short duration does not give sensitive cells sufficient recovery time and hampers their competition against drug-resistant counterparts (Enriquez-Navas et al. 2016). Conversely, prolonged drug administration can lead to the rapid eradication of sensitive cells, accelerating the emergence of drug resistance as is the case with traditional chemotherapy.

We hypothesize that there exists an optimal drug administration duration (t_d) - drug holiday duration (t_h) period pair that maximizes the Time to Treatment Progression (TTP) which is a measure for treatment failure, defined as when 90%

of the simulation space is occupied by cells. This is biologically equivalent to tumor metastasis.

To explore this hypothesis, CancerSim can be employed to conduct numerous trials with different t_d and t_h values for one drug, facilitating a comparison of their performance based on TTP values. The simulation also provides visualizations to help analyze the dynamics of resistant and sensitive cell populations throughout the trials.

5.1.2 Optimal Number of Drugs in an Adaptive Therapy Protocol

Existing computational models have already hinted at the potential advantages of dose modulation in adaptive therapy protocols involving two drugs, showcasing an extended TTP compared to standard treatment (ST) at the Maximum Tolerated Dose (MTD) (D. S. Thomas et al. 2022). To expand upon this, we can use CancerSim to explore whether there exists an optimal number of drugs within the system. Specifically, we can investigate whether cycling through a certain number of drugs can maximize the TTP. Additionally, this experiment can be performed using a combination of multiple drugs in a cocktail setting, where these drugs are administered simultaneously for the same duration.

Our hypothesis suggests that there is an optimal number of drugs within the setup for an adaptive therapy routine. Beyond this optimum, the number of drugs may not improve the TTP.

CancerSim accommodates multiple drugs in adaptive therapy routines, either in combination with other drugs or as standalone treatments. It also models multi-drug resistance, with the fitness costs varying based on the number of resistances a cell possesses. To address this hypothesis, we can maintain constant values for t_d and t_h

and manipulate the number of drugs (n_d) in the adaptive therapy cycle. By observing the dependent variable, TTP, we can estimate the efficiency of different numbers of drugs.

5.1.3 Relation between Spatial Distribution of Resistant Cells and the Success of an Adaptive Therapy Protocol

The emergence of drug resistance is a multifaceted phenomenon within the tumor microenvironment, potentially influenced by factors such as hypoxia (Tredan et al. 2007) and the spatial distribution of drug-resistant cells (Strobl et al. 2022). The distribution of cells surrounding a given cell can significantly impact resource availability. Resistant cells located amidst sensitive cells face stronger spatial competition compared to those scattered throughout the tissue, where they may thrive with limited competition from chemo-sensitive counterparts, leading to their rapid proliferation (Strobl et al. 2022).

In relation, we hypothesize that an adaptive therapy protocol is more likely to succeed if the resistant cell populations are surrounded by sensitive cell populations.

CancerSim can visualize cell populations and distinguish between resistant and sensitive cells. Its visualizer provides insights into tumor dynamics influenced by spatial competition. Additionally, at the end of the simulation, CancerSim can supply data related to the average number of sensitive neighbors for resistant cells. Analyzing the relationship between the TTP and the average number of sensitive cells around resistant cells provides a means to address this research question.

Chapter 6

CONCLUSION

In summary, CancerSim, a three-dimensional agent-based model designed for simulating spatial competition and drug delivery, can serve as a valuable tool for visualizing and analyzing diverse adaptive therapy strategies in the context of cancer. Its ability to model the diffusion of nutrients, drugs, and angiogenic factors, while accurately maintaining their concentrations, strongly positions it as a platform for simulating the spatial competition dynamics of resources in the tumor microenvironment.

Furthermore, we aim to expand the scale of CancerSim simulations. Presently, most runs have employed tissue systems containing 10,000 to 50,000 cells. We aspire to significantly increase the number of cells to approximately 1,000,000, thereby achieving tissue sizes that closely resemble tumors ranging from 1 mm^3 to 1 cm^3 in volume. This scaling up will allow for more realistic and clinically relevant simulations. However, the primary bottleneck in running simulations on a larger scale is the increased computational time for updating the concentration of resources across the tissue. To address it, we would want to look into approximation algorithms that increase the efficiencies of the concentration update operations.

Looking ahead, our future work involves developing experimental designs to execute the experiments outlined in Chapter 5 and using the results to support or challenge our hypotheses.

REFERENCES

Abbott, Robert G., Stephanie Forrest, and Kenneth J. Pienta. 2006. "Simulating the Hallmarks of Cancer." *Artificial Life* 12 (4): 617–634. https://doi.org/10.1162/artl.2006.12.4.617.

Adler, Frederick R., and Deborah M. Gordon. 2019. "Cancer Ecology and Evolution: Positive Interactions and System Vulnerability." *Current opinion in systems biology* 17:1–7. https://doi.org/10.1016/j.coisb.2019.09.001.

Aktipis, C. Athena, and Randolph M. Nesse. 2013. "Evolutionary Foundations for Cancer Biology." *Evolutionary Applications* 6 (1): 144–159. https://doi.org/10.1111/eva.12034.

Angelini, Erin, Yue Wang, Joseph Xu Zhou, Hong Qian, and Sui Huang. 2022. "A Model for the Intrinsic Limit of Cancer Therapy: Duality of Treatment-Induced Cell Death and Treatment-Induced Stemness." *PLOS Computational Biology* 18 (7): e1010319. https://doi.org/10.1371/journal.pcbi.1010319.

Aston, Wayne J., Danika E. Hope, Anna K. Nowak, Bruce W. Robinson, Richard A. Lake, and W. Joost Lesterhuis. 2017. "A Systematic Investigation of the Maximum Tolerated Dose of Cytotoxic Chemotherapy with and without Supportive Care in Mice." *BMC cancer* 17 (1): 684. https://doi.org/10.1186/s12885-017-3677-7.

Bacevic, Katarina, Robert Noble, Ahmed Soffar, Orchid Wael Ammar, Benjamin Boszonyik, Susana Prieto, Charles Vincent, Michael E. Hochberg, Liliana Krasinska, and Daniel Fisher. 2017. "Spatial Competition Constrains Resistance to Targeted Cancer Therapy." *Nature Communications* 8 (1): 1995. https://doi.org/10.1038/s41467-017-01516-1.

Baker, Brendon M., and Christopher S. Chen. 2012. "Deconstructing the Third Dimension – How 3D Culture Microenvironments Alter Cellular Cues." *Journal of Cell Science* 125, no. 13 (July 1, 2012): 3015–3024. https://doi.org/10.1242/jcs.079509.

Beerenwinkel, Niko, Roland F. Schwarz, Moritz Gerstung, and Florian Markowetz. 2015. "Cancer Evolution: Mathematical Models and Computational Inference." *Systematic Biology* 64 (1): e1–e25. https://doi.org/10.1093/sysbio/syu081.

Bonabeau, Eric. 2002. "Agent-Based Modeling: Methods and Techniques for Simulating Human Systems." *Proceedings of the National Academy of Sciences* 99 (suppl_3 2002): 7280–7287. https://doi.org/10.1073/pnas.082080899.

Carslaw, Horatio S., and John C. Jaeger. 1959. *Conduction of Heat in Solids.* 2nd ed. Oxford: Clarendon Press.

Enriquez-Navas, Pedro M., Yoonseok Kam, Tuhin Das, Sabrina Hassan, Ariosto Silva, Parastou Foroutan, Epifanio Ruiz, et al. 2016. "Exploiting Evolutionary Principles to Prolong Tumor Control in Preclinical Models of Breast Cancer." *Science translational medicine* 8 (327): 327ra24. https://doi.org/10.1126/scitranslmed.aad7842.

Farquhar, Cindy, Jane Marjoribanks, Russell Basser, Sarah E. Hetrick, and Anne Lethaby. 2005. "High-dose Chemotherapy and Autologous Bone Marrow or Stem Cell Transplantation versus Conventional Chemotherapy for Women with Metastatic Breast Cancer." *Cochrane Database of Systematic Reviews,* no. 3, https://doi.org/10.1002/14651858.CD003142.pub2.

Gallaher, Jill A., Pedro M. Enriquez-Navas, Kimberly A. Luddy, Robert A. Gatenby, and Alexander R. A. Anderson. 2018. "Spatial Heterogeneity and Evolutionary Dynamics Modulate Time to Recurrence in Continuous and Adaptive Cancer Therapies." *Cancer Research* 78 (8): 2127–2139. https://doi.org/10.1158/0008-5472.CAN-17-2649.

Garattini, Silvio Ken, Debora Basile, Marta Bonotto, Elena Ongaro, Luca Porcu, Carla Corvaja, Monica Cattaneo, et al. 2021. "Drug Holidays and Overall Survival of Patients with Metastatic Colorectal Cancer." *Cancers* 13 (14): 3504. https://doi.org/10.3390/cancers13143504.

Gatenby, Robert A. 2009. "A Change of Strategy in the War on Cancer." *Nature* 459 (7246): 508–509. https://doi.org/10.1038/459508a.

Gatenby, Robert A., Ariosto S. Silva, Robert J. Gillies, and B. Roy Frieden. 2009. "Adaptive Therapy." *Cancer Research* 69, no. 11 (June 1, 2009): 4894–4903. https://doi.org/10.1158/0008-5472.CAN-08-3658.

Hanahan, Douglas, and Robert A. Weinberg. 2011. "Hallmarks of Cancer: The Next Generation." *Cell* 144 (5): 646–674. https://doi.org/10.1016/j.cell.2011.02.013.

Kam, Yoonseok, Tuhin Das, Susan Minton, and Robert A Gatenby. 2014. "Evolutionary Strategy for Systemic Therapy of Metastatic Breast Cancer: Balancing Response with Suppression of Resistance." *Women's health (London, England)* 10 (4): 423–430. https://doi.org/10.2217/whe.14.23.

Korolev, Kirill S., Joao B. Xavier, and Jeff Gore. 2014. "Turning Ecology and Evolution against Cancer." *Nature Reviews Cancer* 14, no. 5 (May): 371–380. https://doi.org/10.1038/nrc3712.

Mallet, D.G., and L.G. De Pillis. 2006. "A Cellular Automata Model of Tumor–Immune System Interactions." *Journal of Theoretical Biology* 239 (3): 334–350. https://doi.org/10.1016/j.jtbi.2005.08.002.

Marusyk, Andriy, Michalina Janiszewska, and Kornelia Polyak. 2020. "Intratumor Heterogeneity: The Rosetta Stone of Therapy Resistance." *Cancer Cell* 37 (4): 471–484. https://doi.org/10.1016/j.ccell.2020.03.007.

Marusyk, Andriy, and Kornelia Polyak. 2010. "Tumor Heterogeneity: Causes and Consequences." *Biochimica et Biophysica Acta (BBA) - Reviews on Cancer* 1805, no. 1 (January 1, 2010): 105–117. https://doi.org/10.1016/j.bbcan.2009.11.002.

McDonald, Thomas O., Yu-Chen Cheng, Christopher Graser, Phillip B. Nicol, Daniel Temko, and Franziska Michor. 2023. "Computational Approaches to Modelling and Optimizing Cancer Treatment." *Nature Reviews Bioengineering,* https://doi.org/10.1038/s44222-023-00089-7.

Metzcar, John, Yafei Wang, Randy Heiland, and Paul Macklin. 2019. "A Review of Cell-Based Computational Modeling in Cancer Biology." *JCO Clinical Cancer Informatics,* no. 3, 1–13. https://doi.org/10.1200/CCI.18.00069.

Norton, Kerri-Ann, Travis Wallace, Niranjan B. Pandey, and Aleksander S. Popel. 2017. "An Agent-Based Model of Triple-Negative Breast Cancer: The Interplay between Chemokine Receptor CCR5 Expression, Cancer Stem Cells, and Hypoxia." *BMC Systems Biology* 11 (1): 68. https://doi.org/10.1186/s12918-017-0445-x.

Nowacka, Marta, Karolina Sterzynska, Malgorzata Andrzejewska, Michal Nowicki, and Radoslaw Januchowski. 2021. "Drug Resistance Evaluation in Novel 3D in Vitro Model." *Biomedicine & Pharmacotherapy* 138:111536. https://doi.org/10.1016/j.biopha.2021.111536.

Robinson, Stewart. 2004. *Simulation: The Practice of Model Development and Use.* Chichester, West Sussex, England ; Hoboken, NJ: John Wiley & Sons, Ltd.

Strobl, Maximilian A. R., Jill Gallaher, Jeffrey West, Mark Robertson-Tessi, Philip K. Maini, and Alexander R. A. Anderson. 2022. "Spatial Structure Impacts Adaptive Therapy by Shaping Intra-Tumoral Competition." *Communications Medicine* 2 (1): 46. https://doi.org/10.1038/s43856-022-00110-x.

Strobl, Maximilian A. R., Jeffrey West, Yannick Viossat, Mehdi Damaghi, Mark Robertson-Tessi, Joel S. Brown, Robert A. Gatenby, Philip K. Maini, and Alexander R. A. Anderson. 2021. "Turnover Modulates the Need for a Cost of Resistance in Adaptive Therapy." *Cancer research* 81 (4): 1135–1147. https://doi.org/10.1158/0008-5472.CAN-20-0806.

Swanton, Charles. 2012. "Intratumour Heterogeneity: Evolution through Space and Time." *Cancer research* 72 (19): 4875–4882. https://doi.org/10.1158/0008-5472.CAN-12-2217.

Tannock, Ian F. 1998. "Conventional Cancer Therapy: Promise Broken or Promise Delayed?" *The Lancet* 351:SII9–SII16. https://doi.org/10.1016/S0140-6736(98)90327-0.

Thomas, Daniel S., Luis H. Cisneros, Alexander R. A. Anderson, and Carlo C. Maley. 2022. "In Silico Investigations of Multi-Drug Adaptive Therapy Protocols." *Cancers* 14 (11): 2699. https://doi.org/10.3390/cancers14112699.

Thomas, Frédéric, Emmanuel Donnadieu, Guillaume M. Charriere, Camille Jacqueline, Aurélie Tasiemski, Pascal Pujol, François Renaud, et al. 2018. "Is Adaptive Therapy Natural?" *PLoS Biology* 16 (10): e2007066. https://doi.org/10.1371/journal.pbio.2007066.

Tredan, O., C. M. Galmarini, K. Patel, and I. F. Tannock. 2007. "Drug Resistance and the Solid Tumor Microenvironment." *JNCI Journal of the National Cancer Institute* 99 (19): 1441–1454. https://doi.org/10.1093/jnci/djm135.

Trisilowati and D. G. Mallet. 2012. "*In Silico* Experimental Modeling of Cancer Treatment." *ISRN Oncology* 2012:1–8. https://doi.org/10.5402/2012/828701.

van Berlo, Damiën, Marjolijn Woutersen, Andre Muller, Marja Pronk, Jelle Vriend, and Betty Hakkert. 2022. "10% Body Weight (Gain) Change as Criterion for the Maximum Tolerated Dose: A Critical Analysis." *Regulatory Toxicology and Pharmacology* 134:105235. https://doi.org/10.1016/j.yrtph.2022.105235.

West, Jeffrey, Fred Adler, Jill Gallaher, Maximilian Strobl, Renee Brady-Nicholls, Joel Brown, Mark Roberson-Tessi, et al. 2023. "A Survey of Open Questions in Adaptive Therapy: Bridging Mathematics and Clinical Translation." *eLife* 12:e84263. https://doi.org/10.7554/eLife.84263.

Wu, Hua-Jun, Daniel Temko, Zoltan Maliga, Andre L. Moreira, Emi Sei, Darlan Conterno Minussi, Jamie Dean, et al. 2022. "Spatial Intra-Tumor Heterogeneity

Is Associated with Survival of Lung Adenocarcinoma Patients." *Cell Genomics* 2 (8): 100165. https://doi.org/10.1016/j.xgen.2022.100165.

Yu, Jessica S., and Neda Bagheri. 2020. "Agent-Based Models Predict Emergent Behavior of Heterogeneous Cell Populations in Dynamic Microenvironments." *Frontiers in Bioengineering and Biotechnology* 8.

Zhang, Jingsong, Jessica J. Cunningham, Joel S. Brown, and Robert A. Gatenby. 2017. "Integrating Evolutionary Dynamics into Treatment of Metastatic Castrate-Resistant Prostate Cancer." *Nature Communications* 8, no. 1 (November 28, 2017): 1816. https://doi.org/10.1038/s41467-017-01968-5.